Journal of Renewable Materials

Tech Science Press

DOI: 10.32604/jrm.2024.057419

ARTICLE

Microwave-Assisted Acetylated Lignin Loaded into Cellulose Acetate for Efficient UV-Shielding Films

Ahmed M. Khalil[1] and Samir Kamel[2,*]

[1]Photochemistry Department, National Research Centre, Giza, 12622, Egypt

[2]Cellulose and Paper Department, National Research Centre, Giza, 12622, Egypt

[*]Corresponding Author: Samir Kamel. Email: samirki@yahoo.com

Received: 16 August 2024 Accepted: 01 November 2024 Published: 20 February 2025

ABSTRACT

Developing favorable bio-based polymers that replace petroleum-based plastics is an essential environmental demand. Lignin is a by-product of the chemical pulping industry. It is a natural UV protection ingredient in broad-spectrum (UVA and UVB) sunscreens. It could be partially and selectively acetylated in a simple, fast, and more reliable process. In this work, a composite film was prepared with UV-resistant properties through a casting method. Bio-based cellulose acetate (CA) was employed as a major matrix while nano-acetylated kraft lignin (AL-NPs) was used as filler during synthesizing UV-shielding films loaded with various amounts (1–5 wt.%) of AL-NPs. Kraft lignin was acetylated through a simple and fast microwave-assisted process using acetic acid as a solvent and acetylating agent. The physicochemical and morphological characteristics of the prepared films were evaluated using different methods, including scanning electron microscopy (SEM), Fourier Transform Infrared Spectroscopy (FTIR), X-ray diffraction analysis (XRD), mechanical testing and contact angle measurement. The UV-Vis spectroscopy optical investigation of the prepared films revealed that AL-NPs in the CA matrix showed strong UV absorption. This feature demonstrated the effectiveness of our research in developing UV-resistant bio-based polymer films. Hence, the prepared films can be considered as successful candidates to be applied in packaging applications.

KEYWORDS

Cellulose acetate; microwave-assisted acetylation; nano lignin acetate; UV-shielding

1 Introduction

During the day, the skin is continuously exposed to various solar radiation wavelengths. UVA (315–400 nm) and UVB (280–315 nm) are biologically important, accounting for 3% of solar energy that reaches the Earth's surface [1]. The ozone layer in the atmosphere filters off any wavelength less than 290 nm, including the short UVB spectrum and UVC (200–280 nm). The artificially produced UVC may be highly mutagenic or fatal upon high exposure. In contrast to UVB, UVC from artificial sources only slightly damages the skin's viable areas because the stratum corneum absorbs it within the outermost nonviable epidermal layer [2]. The main harmful effects of ultraviolet radiation (UVR) are known to include autoimmune disorders, skin aging, cancer and eye impairment. The beneficial contribution of

UVR to the regulation of homeostasis is unappreciated, except for UVB's necessity for synthesizing vitamin D3 [3].

The recent discovery of the potency of agro-polymer-based materials has ignited a wave of optimism. Their wide availability, biodegradability, renewability and biocompatibility allow them to be promising avenues for the future of UV protection [4]. Among the common biopolymers; cellulose and lignin are considered with their agricultural origin. They have captured the attention of researchers to produce bio-based composites [5]. Cellulose, with its natural abundance and biocompatibility stands out from synthetic materials [6]. Its facile conversion into various well-soluble and processable derivatives adds to its intrigue [7–9]. On the other hand, lignin is a by-product of the pulp and paper industries alongside bio-refining processes. It is the most popular natural phenolic biopolymer on the market. Over 50 million tons are produced annually worldwide [10]. Moreover, lignin has low cytotoxicity, biodegradability, antimicrobial, antioxidant, anti-inflammatory, and UV-blocking properties [11–13]. 1%–2% of the produced lignin is converted into value-added products [14]. It has functional groups called chromophores, including methoxy-substituted phenoxy and quinones groups. These groups can be conjugated with double bonds or carbonyl functional groups to absorb UV radiation with a wavelength range of 250–400 nm [15]. The unsaturated groups absorb visible light, making lignin's color brownish to black [16]. The exposure of lignin to photo-irradiation turns it into a dark color. This behavior positively affects the application of lignin as a UV-blocker. The resulting darkness in its color is due to light-catalyzed photo-reactions with lignin chromophores formed of quinones and other chromophoric groups. The dark color of lignin is a challenge has to be solved for its application. To minimize this issue, lignin was modified through acetylation [17] and fractionation to discolored fractions of lignin for reducing its color without affecting its UV absorption [18]. Regarding the selective chemical modification of hydroxyl groups in the lignin, only a few papers described this point. Monteil-Rivera et al. [19] reported that through a microwave-assisted, solvent and catalyst-free process, maleic anhydride can react with the aliphatic hydroxyl groups of lignin. Ye et al. [20] described a selective aminolysis of acetylated lignin by releasing the phenolic hydroxyls and maintaining the acetylated aliphatic hydroxyl groups. Interestingly, in that work, the authors reported that partially acetylated lignin simultaneously improved the thermo-oxidative stability of propylene and maintained its mechanical properties. Oliveira et al. [21] demonstrated that partial and selective lignin acetylation can be carried out through a fast microwave-assisted process to be a greener and simpler process using acetic acid as an acetylating agent and solvent. Cellulose-based films containing UV-blockers, as an alternative to synthetic polymers, have been reported to have a wide range of applications. They include outdoor UV-sensitive polymers [22], clean windows [23], car windshields [24], and contact lenses [25]. For instance, significant UV absorbance enhancements were reported by adding lignin to commercial sunscreen products. Studies of lignin-cellulose films have focused on utilizing raw lignin as a UV-blocker. Kraft lignin was added to transparent and flexible gellan gum and 2-hydroxyethyl cellulose film for food packaging [26] and biomedical [27] applications, respectively. Acetylated lignin was used as an anticorrosive and UV-blocking epoxy resin [28]. Yang et al. found that the immobilization of microorganisms by lignin maintained high biological activity [29].

Compared to conventional heating processes, microwave nonconventional heating is more energy-efficient. This character is due to its merits of volumetric, high yields, rapid, selective heating, and high product purities because of reduced side reactions [30]. Nonconventional microwave heating was applied as a selective esterification of various carboxylic acids [31], functionalization of cellulose in an ionic liquid [32], and esterification of lignin with various anhydrides (propionic, acetic, maleic, methacrylic, butyric) without using a catalyst and being a solvent-free process. It was found that the microwave-assisted esterification of lignin accelerated the reaction rate by 3000 times compared to conventional heating [19]. Yao et al. prepared acetylated and hexanoated lignin with high degrees of substitution, 97% and 98%, respectively, using solvent and catalyst-free microwave-assisted [33]. Based on this concept, the

present study showed the preparation of acetylated lignin (AL) preparation through fast, simple, and appropriate microwave-assisted methodology using acetic acid as solvent and acetylating agent. For enhancing the miscibility and interaction of AL with CA, the prepared AL was dissolved in methanol and precipitated as nano-acetylated lignin (AL-NPs) in water. Homogenous cellulose acetate (CA) films were prepared as a reference material and films were loaded with AL-NPs. The CA and CA/AL-NPs films were cast and characterized for their structural, UV-blocking, and hydrophobic properties to be utilized as packaging films.

2 Materials and Methods

2.1 Materials

The black liquor was gently supplied by Quena Company of Paper Industry, Egypt. Cellulose acetate (CA) was purchased from (Fluke Biochemical Co., Schaffhausen, Switzerland) (M. wt: 37,000 g/mol, CAS number: 9004-35-7, purity = 40% acetyl groups). All chemicals were used as received: sulfuric acid (98%, Synth, Brazil) and glacial acetic acid (Synth, Sao Paulo, Brazil).

2.2 Methods

2.2.1 Lignin Separation

The lignin separation method was employed to isolate lignin from the black liquor. The black liquor was concentrated using a rotary evaporator. The solution's pH was adjusted to 1.0 using concentrated HCl. Lignin, as a precipitated solid was separated by centrifugation. The solid lignin was washed until its pH reached 2.0 then dried.

2.2.2 Microwave-Assisted Acetylation of Lignin and Conversion to Nano-Form

2 g lignin was dissolved in a 100 mL solution of glacial acetic acid and 1% (v/v) of H_2SO_4 as a catalyst by magnetic stirring at room temperature. The acetylation was performed under reflux in a domestic microwave (700 W) for 5 min as reaction time, giving acetylated lignin (AL). To get nano acetylated lignin, it was dissolved in methanol using a magnetic stirrer. It was poured into 400 mL cold water and stirred for 1 h until lignin precipitation. The nano-acetylated lignin (AL-NPs) was filtered and washed with distilled water until neutrality.

2.2.3 Preparation of Films (CA/AL-NPs)

The preparation of CA and CA/AL-NPs films was carried out according to the following steps. Solutions of CA were meticulously prepared by dissolving them in 20 mL of acetone. The required amount of AL-NPs in water was sonicated for 5 min using an ultrasonic dropper. The sonicated AL-NPs solution was added to the CA solution and stirred using a magnetic stirrer for 5 min. Glycerol was added as a plasticizer during stirring, then poured onto a Teflon petri dish and annealed at 50°C in a vacuum oven. Plain CA film was also fabricated using the same procedure and considered as the reference film. The coded films are CA, CA/AL-NPs 0.5%, CA/AL-NPs 1%, CA/AL-NPs 2%, and CA/AL-NPs 5% related to weight % of AL-NPs such as 0, 0.5, 1, 2, and 5, respectively.

2.3 Characterization

2.3.1 Fourier Transforms Infrared Spectroscopy–Attenuated Total Reflectance (FTIR–ATR)

The Fourier transform infrared spectrometer (JASCO, Tokyo, Japan) was used to measure the FTIR spectra of L and ALNPs. This method is crucial in identifying the functional groups present in the samples, providing valuable information about their chemical composition. These samples were prepared and pressed in a KBr disc, ensuring uniformity and consistency in the measurements. The ATR spectra of CA/AL-NPs films were also investigated. The measurements were taken in the range of 400–4000 cm^{-1}.

2.3.2 Surface Morphology

The particle size of the prepared AL-NPs was studied using an STA6000, Perkin Elmer (USA), at an acceleration voltage of 120 kV.

The surface morphology of CA and CA/AL-NPs films was performed on a scanning electron microscope (FEI IN SPECTS Company, Philips, Holland) operating at 10–15 kV. The fractured surfaces of the investigated film samples were cut under liquid nitrogen. They were coated with an ultrathin gold layer in a sputter coating system.

2.3.3 X-Ray Diffraction Analysis (XRD)

The XRD patterns of CA and CA/AL-NPs films were investigated using a Diano X-ray diffractometer. This device used a CuKα radiation source (λ = 0.15418 nm) energized at 45 kV. The diffraction angle (2θ) ranged from 10 to 80° in reflection mode.

2.3.4 Contact Angle

Hydrophobic measurements as water-contacting angles of the fabricated films were determined under the ASTM (D-7334) standard test using GA-1102 Optical Contact Angle, Hunan Gonoava Instrument Co. Ltd. (Changsha, China).

2.3.5 Mechanical Properties

The mechanical strength was characterized by a Zwick tensile testing machine Z010 at ASTM D638, which was used to observe the tensile strength and elongation % of the fabricated films.

2.3.6 UV-Vis Investigation

The optical properties of CA/AL-NPs films were investigated using a Spectrophotometer JASCO (V-570) with a spectral range from 200 to 700 nm.

3 Results and Discussion

3.1 Overview of Lignin Acetylation and Conversion to Nano-Form

Lignin was hydrophobized via acetylation of its hydroxyl groups to increase the interfacial adhesion with cellulose acetate (CA). This step was carried out via a nucleophilic attack on the -C=O of the acetic anhydride by the hydroxyl group ion pair of lignin (Scheme 1). Microwave radiation can enhance yields with reducing reaction times without additional solvents. Importantly, this process is easy to work up, providing reassurance about its practicality [19]. For more dispersion of AL, AL-NPs were prepared based on the hydrophobicity nature of the AL. The latter was dissolved in methanol and gradually dropped to water with stirring. As lignin is water-immiscible, AL began to associate as spheres to minimize hydrophobic interactions forming nanometric size particles such as nano-acetylated lignin (AL-NPs).

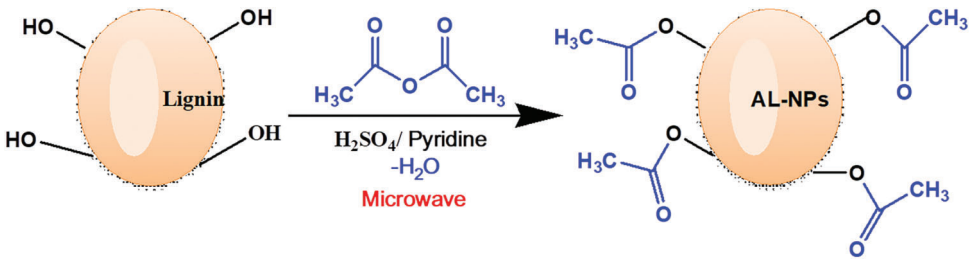

Scheme 1: Microwave acetylation of lignin

3.2 Fourier Transform Infrared Spectroscopy (FTIR) of Lignin, AL-NPs and Their Films

Our investigation into the structural properties of lignin and AL-NPs, conducted with FTIR analysis, has led to some findings. Fig. 1a shows the FTIR spectra of unmodified lignin and AL-NPs obtained by refluxing in a domestic microwave at 700 W for 5 min. The unmodified lignin displays typical lignin characteristics in broad bands at 3000–3500 cm^{-1} (OH stretch), with distinct bands at 2934 cm^{-1} (CH stretch), 1599, 1512, 1454, 1421 cm^{-1} (aromatic skeletal vibrations), 1213 cm^{-1} (C-O stretch), and 1038 cm^{-1} (aromatic in plane C-H deformation) cm^{-1} [34,35]. The modified lignins (AL-NPs) show clear evidence of acetylation, with new major signals at 1607 cm^{-1} corresponding to the aliphatic C=O stretch band in ester groups [19]. In addition, the absence of the aromatic C=O stretch band at a wavenumber greater than 1760 cm^{-1}, as per the literature, suggests selective acetylation in the aliphatic hydroxyl groups [21]. The decreasing absorption intensity and brooding of the OH peak and a new peak appearing at 1372 cm^{-1} denote the stretching C-H of the acetate group, indicating the esterification of OH groups.

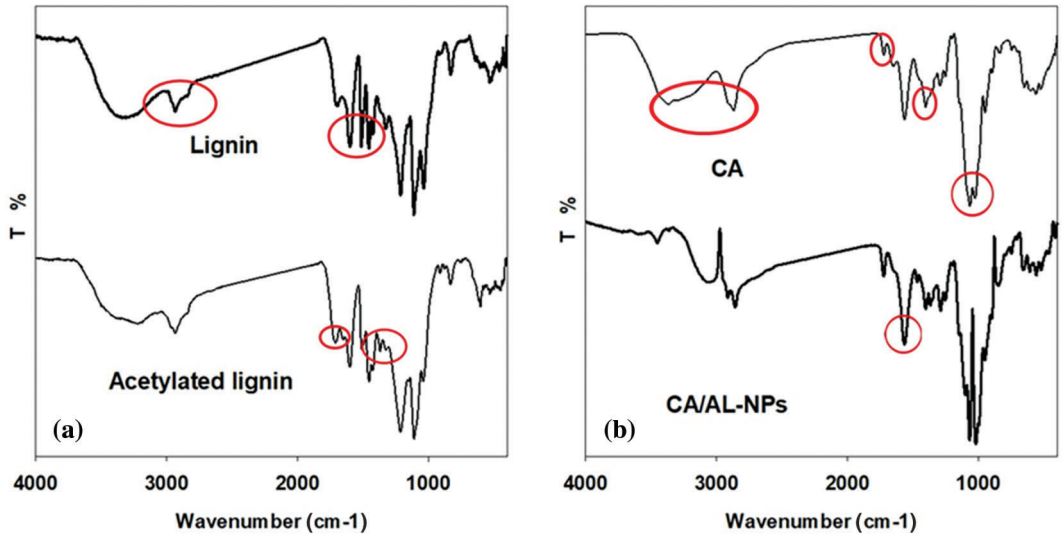

Figure 1: FTIR spectra of (a) lignin and AL-NPs and (b) ATR spectra of CA and CA/AL-NPs films

The impact of AL-NPs loading onto the CA film structure was investigated using ATR-FTIR spectroscopy. The films obtained from 0% and 10% AL-NPs were considered representative films, and their ATR spectra are presented in Fig. 1b. For CA, characteristic IR peaks are observed at 3300 cm^{-1} for -OH, 2931 cm^{-1} for -CH, and 1748 cm^{-1} for C=O groups. The CH_2- group displays a peak at 1416 cm^{-1}, which could be accompanied by vibrational C-O-C binding and stretching modes of the CH_3 groups of CA radicals. A peak at 1056 cm^{-1} indicates a stretching C-O bond. Upon loading AL-NPs into the CA matrix, the majority of the previously investigated peaks of CA and AL-NPs overlap. This overlap indicates a significant interaction between CA and AL-NPs. However, after loading of AL-NPs into the CA matrix, the peak intensity at 1568 cm^{-1}, which refers to the aromatic structure of lignin, was increased due to its overleaping with the characteristic peak of the -COOH in CA [36].

3.3 Morphological Investigation via TEM and SEM Techniques

The nano-acetylated lignin (AL-NPs) was successfully prepared through precipitation in methanol. The dissolved AL was analyzed by Transmission electron microscopy (TEM) as shown in Fig. 2. TEM is used in wood and fiber research for visualizing their nanoparticle sizes and structures [37]. Fig. 2a shows a TEM image for AL-NPs. Dark spots in images are AL-NPs which are uniformly dispersed in the CA matrix (brighter background in images). From the selected area electron diffraction (SAED) pattern in Fig. 2b,

the prepared nanoparticles show a major amorphous structure with few crystalline regions. The average size of AL-NPs lies in the range of 25–40 nm as shown in Fig. 2c. It can be noticed that there is a change in the particle size. It depends on the followed process of synthesis of these nanoparticles leading to an anticipated 'nano' impact in the formed film composites. Some emerging variations in the characteristics of the formed composites may arise due to the high surface area of AL-NPs and the small distances between these nanoparticles at any AL-NPs concentrations.

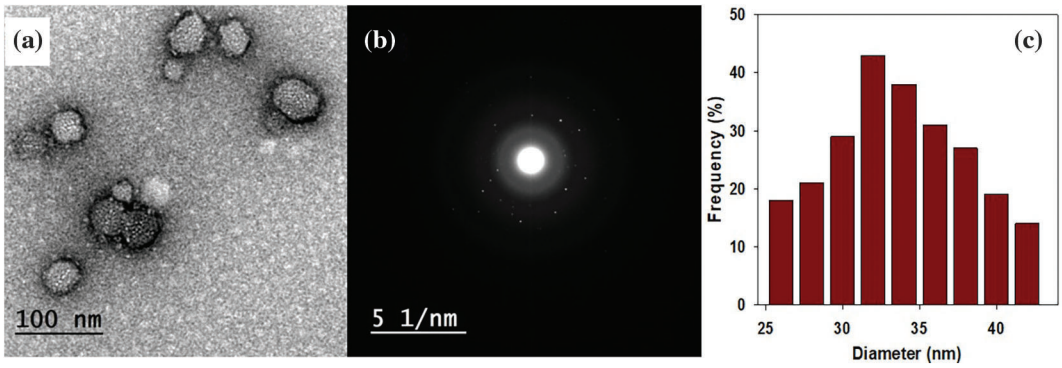

Figure 2: (a) Transmission electron microscopy (TEM) image, (b) SAED, and (c) Particle size distribution of AL-NPs

Among the challenges to producing homogenous films is to obtain an acceptable adhesion between the polymer and filler which has to be well spread in the polymeric matrix. AL-NPs showed to be efficient with enhancing the affinity of this filler with the major cellulosic material. Fig. 3a illustrates the scanning electron microscopy (SEM) micrograph for CA. The image displays the surface morphology of CA with a uniform surface having some roughness. Upon introducing AL-NPs into CA, some particles appear in a spherical structure. They have various sizes extending through the major polymeric matrix as demonstrated in Fig. 3b. AL-NPs are present as small beads in the polymeric matrix. After acetylating lignin, hydrogen bonds have been abstracted producing a characteristic hydrophobic morphology for these nanoparticles. The acetylation step of lignin assisted in enhancing its compatibility with the CA matrix.

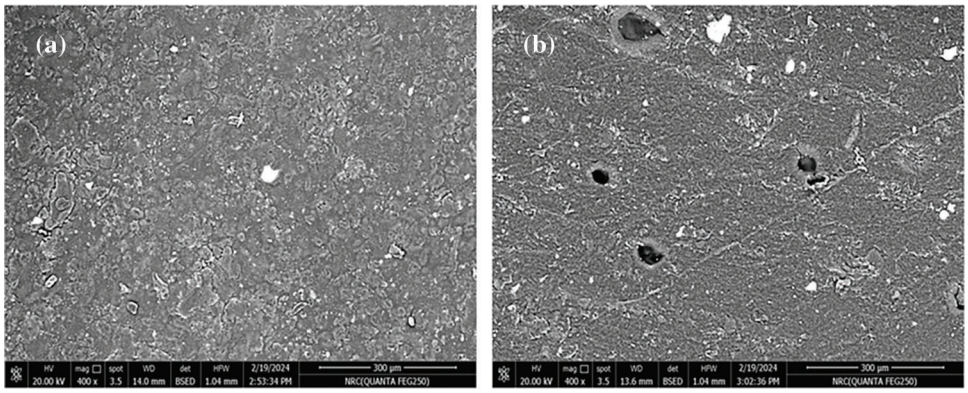

Figure 3: SEM images of (a) CA and (b) CA/AL-NPs films

3.4 X-Ray Diffraction Analysis of Films

The X-ray diffraction (XRD) technique, a comprehensive tool, was used in this study to monitor the alteration in the crystalline nature of the investigated films. In addition, it plays a crucial role in our

understanding of the effects of AL-NPs loading onto the CA film structure. Fig. 4 demonstrates the patterns of pure cellulose acetate when blended with different contents of AL-NPs. A sharp peak can be observed at 2θ = 19.7° for pure CA. The process of synthesizing AL-NPs contributes to some shifts in the amorphous regions. Hence, partial crystalline forms may arise. A peak is noticed at (2θ) 20.8° corresponding to the 002 plane. Another corresponding broad peak for lignin appears at 2θ = 40.3° [38]. It had broadened due to blending ACL-NPs with CA.

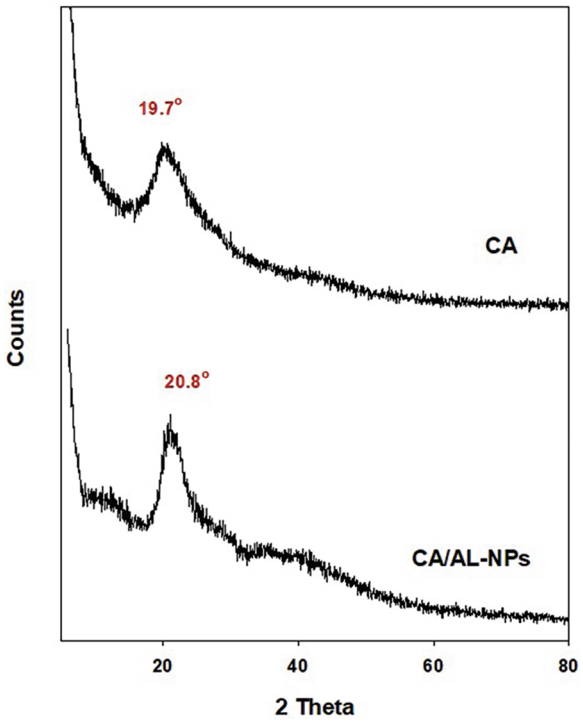

Figure 4: XRD spectra of CA and CA/AL-NPs films

3.5 Hydrophobic Characterization

The contact angle measurements of CA and CA/AL-NPs fabricated films were carried out to recognize the wettability of the surfaces. The results are shown in Fig. 5. For CA film, a wetting feature can be affirmed due to the presence of a hydroxyl functional group. This group is liable for hydrophilicity and its affinity with water. Hence, it expresses a hydrophilic behavior for CA with a contact angle of 49°. Upon introducing AL-NPs to CA, the contact angle measurements tended to increase. This behavior refers to the hydrophobic nature of the analyzed nanocomposites. The nature of both components can denote the growth in these contact angle values: the hydrophilic CA and the hydrophobic AL-NPs [39]. Contact angle values indicate that the tested films loaded with AL-NPs possess higher measurements than CA. Loading AL-NPs into CA to form the investigated films enhanced the bioplastic's hydrophobic properties, pointing to a noticeable retraction in the hydrophobic nature of these CA-based films. This trait is accompanied by a proportional increment in contact angle readings, elevating AL-NPs content. Among the major functional groups of lignin, phenolic OH is considered. During acetylation, these hydroxyls are replaced with $-COCH_3$ as a nonpolar group. The latter promotes the hydrophobic nature of AL-NPs with acceptable solubility in organic solvents. The main hydrophobic character is achieved with the more hydrophobic AL-NPs rather than CA, which contains the more polar OH groups. The rise in the hydrophobicity of the fabricated films showed superior water-resistant characteristics [40].

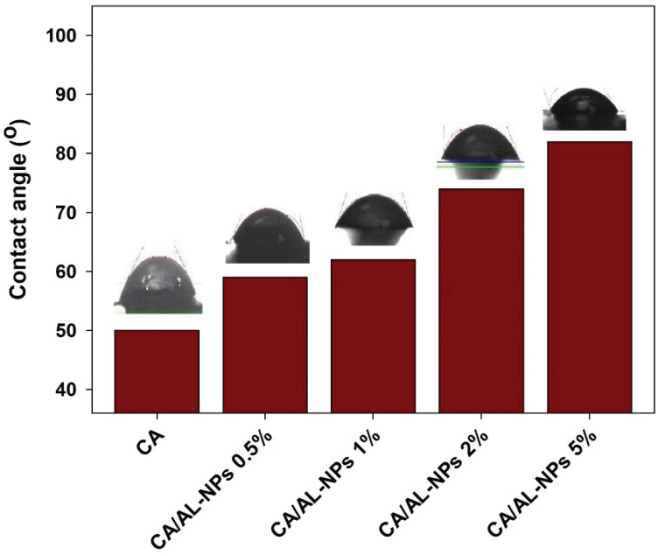

Figure 5: Contact angles of CA and CA/AL-NPs films

3.6 Mechanical Study

The primary focus of this study was to determine the impact of loading AL-NPs on the tensile characteristics of the CA film. The investigation of tensile strength (TS) and elongation %, as depicted in Fig. 6, revealed that these properties are dependent on the strength of CA in relation to the dispersion of AL-NPs within the polymeric matrix. The comparison of the TS of the virgin CA film with its AL-NPs loaded counterparts, as shown in Fig. 6a, demonstrated a proportional increase with the addition of AL-NPs, reaching a stabilized value for the CA/AL-NPs 2%. A subsequent decrease was observed with higher AL-NP content. This significant increase in TS can be attributed to the strong interaction between the CA and AL-NPs. However, the stiffness of the cellulosic structure of AL-NPs led to a noticeable decrement in TS values for these composites upon loading higher AL-NPs concentration (5%) [41]. The previous values demonstrated that loading these nanoparticles to CA boosted the TS of the tested films, indicating a strong compatibility between CA and AL-NPs. Moreover, there is an effective shift in the stress from the polymer to AL-NPs [42]. This transfer led to elevating the TS of the tested films. The elongation % of the investigated films showed a diminishing behavior, as displayed in Fig. 6b. This decrement may be referred to as reduced polymeric mobility because of the stiff AL-NPs.

3.7 UV-Blocking Capacity

Sunlight radiation of UVA and UVB contributes in decomposing organic compounds and discoloration of dyes. Moreover, polymers may damage as a result of prolonged exposure to UV irradiation. UV absorbers/blockers are essential to diminish the deteriorating photo-effects. In this study, a UV-Vis spectrophotometer was used to measure the transmittance of the fabricated films at wavelengths ranging from 200 to 700 nm (Fig. 7). As lignin is involved in composites, we believe that it supplies considerable ultraviolet blocking features. The results revealed that it provides high protection against UVA (320–400 nm) and UVB radiation (280–320 nm) [38]. CA/AL-NPs films have shown higher protection against UV radiation when compared to CA film. Increasing the AL-NPs increased the UV-blocking capability. Nearly more than 90% of UVA and UVB rays have been blocked.

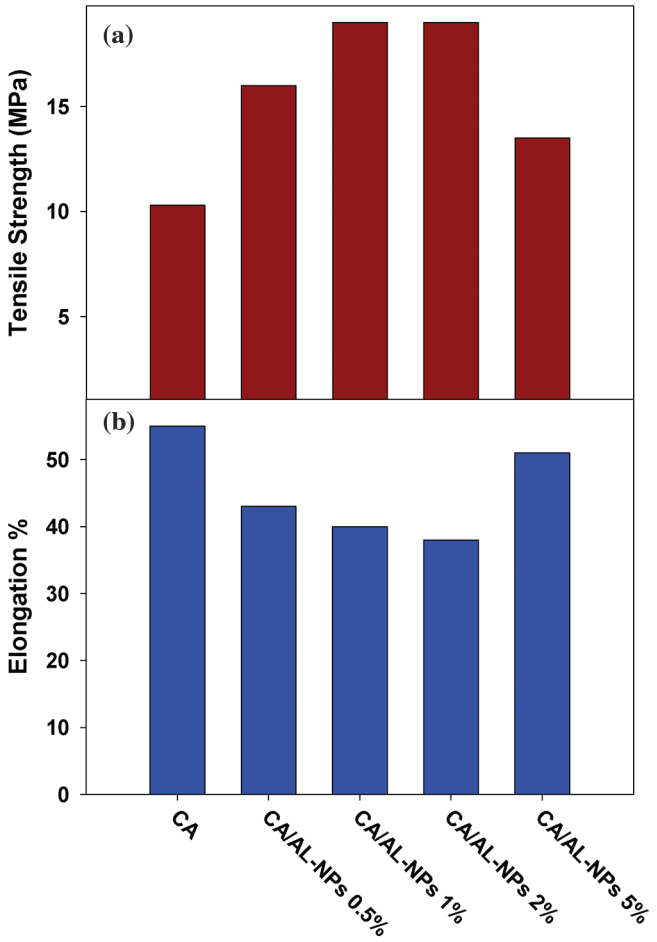

Figure 6: Tensile strength (a) and elongation % (b) of CA and CA/AL-NPs films

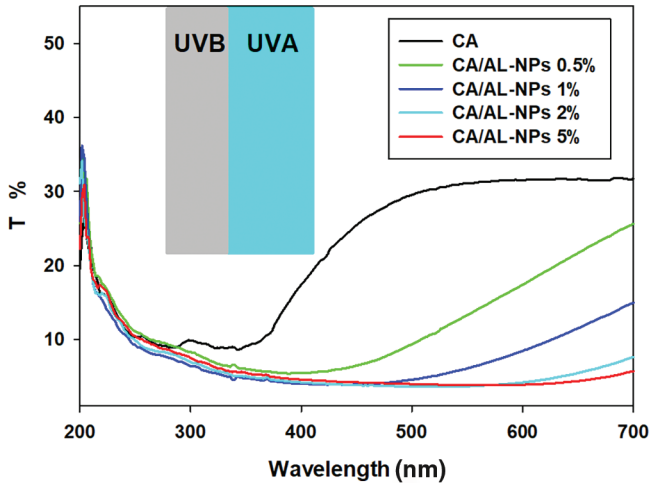

Figure 7: UV-Vis spectra of CA and CA/AL-NPs films

4 Conclusion

In this study, a microwave-assisted process using acetic acid as an acetylating agent was successfully used for acetylating lignin, followed by conversion into nano-forms. Using the solution casting approach, cellulose acetate films loaded with different concentrations (0–5 wt.%) of nano-acetylated lignin were created. The acetylated lignin, which could act as sacrificial hydrogen, was uniformly distributed in the fabricated films. The wettability study tended towards hydrophobia with the addition of acetylating lignin, which can be explained by the hydrophilic nature of cellulose acetate and the hydrophobic nature of acetylating lignin. The film's hydrophobic properties increased with a higher percentage of acetylating lignin. The mechanical study has highlighted the significant increase in tensile strength with the addition of nano-acetylated lignin, the effective shift in stress from the polymer to nano-acetylated lignin, and the reduction in elongation % due to the presence of stiff nano-acetylated lignin. Moreover, UV-Vis demonstrates that the transmittance of pure cellulose acetate film declines as nano-acetylated lignin is added. The prepared films loaded with nano-acetylated lignin reduced light transmission with high protection, more than 90%, against UVA and UVB radiation. Accordingly, these films can be used as UV blocker packaging films.

Acknowledgement: The authors appreciate the National Research Centre (NRC)—Egypt for the financial support of this research activity.

Funding Statement: This research received no external funding.

Author Contributions: Ahmed M. Khalil and Samir Kamel have the same contribution in conceptualization, draft preparation, writing, and editing. All authors reviewed the results and approved the final version of the manuscript.

Availability of Data and Materials: Not applicable.

Ethics Approval: Not applicable.

Conflicts of Interest: The authors declare no conflict of interest to report in the present study.

References

1. Slominski AT, Zmijewski MA, Plonka PM, Szaflarski JP, Paus R. How UV light touches the brain and endocrine system through skin, and why. Endocrinology. 2018;159(5):1992–2007. doi:10.1210/en.2017-03230.
2. Busch L, Kröger M, Zamudio Díaz DF, Schleusener J, Lohan SB, Ma J, et al. Far-UVC-and UVB-induced DNA damage depending on skin type. Exp Dermatol. 2023;32(9):1582–7. doi:10.1111/exd.v32.9.
3. Slominski RM, Chen JY, Raman C, Slominski AT. Photo-neuro-immuno-endocrinology: how the ultraviolet radiation regulates the body, brain, and immune system. Proc Nat Acad Sci. 2024;121(14):e2308374121. doi:10.1073/pnas.2308374121.
4. Akhtar S, Gupta AK, Kumar H. Manufacturing and applications of cellulosic films in packaging: an alternative for plastic films. Current Nut Food Sci. 2024;20(4):384–400. doi:10.2174/1573401319666230609140552.
5. Cheng W, Zhu Y, Jiang G, Cao K, Zeng S, Chen W, et al. Sustainable cellulose and its derivatives for promising biomedical applications. Prog Mater Sci. 2023;138:101152. doi:10.1016/j.pmatsci.2023.101152.
6. Abdelhamid AE, Khalil AM. Polymeric membranes based on cellulose acetate loaded with candle soot nanoparticles for water desalination. J Macromol Sci. 2019;56(2):153–61. doi:10.1080/10601325.2018.1559698.
7. Hasanin MS, Abdelhameed RM, Abbas H, Ibrahim S. Photocatalytic degradation of hazard migrated compound from food packaging materials using antimicrobial strontium titanate incorporated cellulose acetate. J Photochem Photobio A: Chem. 2024;447:115223. doi:10.1016/j.jphotochem.2023.115223.

8. Huang X, Huang R, Zhang Q, Zhang Z, Fan J, Huang J. Cellulose-based biomass composite films for plastic replacement: synergistic UV shielding, antibacterial and antioxidant properties. Int J Biol Macromol. 2024;270:132418. doi:10.1016/j.ijbiomac.2024.132418.
9. Huang X, Huang R, Zhang Q, Zhang Z, Fan J, Huang J. Preparation of a cellulose-based biomass film with antibacterial and high UV-shielding properties. Ind Crops Prod. 2024;212:118301. doi:10.1016/j.indcrop.2024.118301.
10. El-Sayed NS, Hasanin M, Kamel S. Wood by-products as UV protection: a consequence review. J Renew Mat. 2024;12(4):699–720. doi:10.32604/jrm.2024.049118.
11. Gil-Chávez GJ, Padhi SSP, Pereira CV, Guerreiro JN, Matias AA, Smirnova I. Cytotoxicity and biological capacity of sulfur-free lignins obtained in novel biorefining process. Int J Biol Macromol. 2019;136:697–703. doi:10.1016/j.ijbiomac.2019.06.021.
12. Gordobil O, Herrera R, Yahyaoui M, İlk S, Kaya M, Labidi J. Potential use of kraft and organosolv lignins as a natural additive for healthcare products. RSC Adv. 2018;8(43):24525–33. doi:10.1039/C8RA02255K.
13. Barapatre A, Meena AS, Mekala S, Das A, Jha H. *In vitro* evaluation of antioxidant and cytotoxic activities of lignin fractions extracted from *Acacia nilotica*. Int J Biol Macromol. 2016;86:443–53. doi:10.1016/j.ijbiomac.2016.01.109.
14. Rinaldi R, Jastrzebski R, Clough MT, Ralph J, Kennema M, Bruijnincx PC, et al. Paving the way for lignin valorisation: recent advances in bioengineering, biorefining and catalysis. Angew Chem Int Ed. 2016;55(29):8164–215. doi:10.1002/anie.v55.29.
15. Sadeghifar H, Ragauskas A. Lignin as a UV light blocker—a review. Polymers. 2020;12(5):1134. doi:10.3390/polym12051134.
16. Paulsson M, Parkås J. Light-induced yellowing of lignocellulosic pulps-mechanisms and preventive methods. BioResources. 2012;7(4):5995–6040.
17. Zhang H, Liu X, Fu S, Chen Y. High-value utilization of kraft lignin: color reduction and evaluation as sunscreen ingredient. Int J Biol Macromol. 2019;133:86–92. doi:10.1016/j.ijbiomac.2019.04.092.
18. Parit M, Saha P, Davis VA, Jiang Z. Transparent and homogenous cellulose nanocrystal/lignin UV-protection films. ACS Omega. 2018;3(9):10679–91. doi:10.1021/acsomega.8b01345.
19. Monteil-Rivera F, Paquet L. Solvent-free catalyst-free microwave-assisted acylation of lignin. Ind Crops Prod. 2015;65:446–53. doi:10.1016/j.indcrop.2014.10.060.
20. Ye D, Kong J, Gu S, Zhou Y, Huang C, Xu W, et al. Selective aminolysis of acetylated lignin: toward simultaneously improving thermal-oxidative stability and maintaining mechanical properties of polypropylene. Int J Biol Macromol. 2018;108:775–81. doi:10.1016/j.ijbiomac.2017.10.168.
21. de Oliveira DR, Avelino F, Mazzetto SE, Lomonaco D. Microwave-assisted selective acetylation of Kraft lignin: acetic acid as a sustainable reactant for lignin valorization. Int J Biol Macromol. 2020;164:1536–44. doi:10.1016/j.ijbiomac.2020.07.216.
22. Lawrynowicz A, Vuori S, Palo E, Winther M, Lastusaari M, Miettunen K. Transforming fabrics into UV-sensing wearables: a photochromic hackmanite coating for repeatable detection. Chem Eng J. 2024;494:153069.
23. Song Y, Xu Y, Li D, Chen S, Xu F. Sustainable and superhydrophobic lignocellulose-based transparent films with efficient light management and self-cleaning. ACS Appl Mater Interfaces. 2021;13(41):49340–7. doi:10.1021/acsami.1c14948.
24. Harun-Ur-Rashid M, Imran AB, Susan MABH. Green polymer nanocomposites in automotive and packaging industries. Curr Pharm Biotechnol. 2023;24(1):145–63. doi:10.2174/1389201023666220506111027.
25. Kang M, Oderinde O, Han X, Fu G, Zhang Z. Development of oxidized hydroxyethyl cellulose-based hydrogel enabling unique mechanical, transparent and photochromic properties for contact lenses. Int J Biol Macromol. 2021;183:1162–73. doi:10.1016/j.ijbiomac.2021.05.029.
26. Rukmanikrishnan B, Ramalingam S, Rajasekharan SK, Lee J, Lee J. Binary and ternary sustainable composites of gellan gum, hydroxyethyl cellulose and lignin for food packaging applications: biocompatibility, antioxidant activity, UV and water barrier properties. Int J Biol Macromol. 2020;153:55–62. doi:10.1016/j.ijbiomac.2020.03.016.

27. Luzi F, Yang W, Ma P, Torre L, Puglia D. Lignin-based materials with antioxidant and antimicrobial properties, Lignin-based materials for biomedical applications. Amsterdam, The Netherlands: Elsevier; 2021. p. 291–326.
28. Diógenes OB, de Oliveira DR, da Silva LR, Pereira ÍG, Mazzetto SE, Araujo WS, et al. Development of coal tar-free coatings: acetylated lignin as a bio-additive for anticorrosive and UV-blocking epoxy resins. Prog Org Coat. 2021;161:106533. doi:10.1016/j.porgcoat.2021.106533.
29. Yang J, Xing S, Yang W, Zhang A, Wang W. Application potential of modified waste-lignin as microbial immobilization carriers for improve soil fertility. React Funct Polym. 2021;196:105837.
30. Wang N, Xu A, Liu K, Zhao Z, Li H, Gao X. Performance of green solvents in microwave-assisted pretreatment of lignocellulose. Chem Eng J. 2024;482:148786. doi:10.1016/j.cej.2024.148786.
31. Pathak G, Das D, Rokhum SL. A microwave-assisted highly practical chemoselective esterification and amidation of carboxylic acids. RSC Adv. 2016;6(96):93729–40. doi:10.1039/C6RA22558F.
32. Possidonio S, Fidale LC, El Seoud OA. Microwave-assisted derivatization of cellulose in an ionic liquid: an efficient, expedient synthesis of simple and mixed carboxylic esters. J Poly Sci Part A: Poly Chem. 2010;48(1):134–43. doi:10.1002/pola.v48:1.
33. Yao J, Odelius K, Hakkarainen M. Microwave hydrophobized lignin with antioxidant activity for fused filament fabrication. ACS Appl Poly Mat. 2021;3(7):3538–48. doi:10.1021/acsapm.1c00438.
34. Nada A-AM, El-Sakhawy M, Kamel SM. Infra-red spectroscopic study of lignins. Poly Degrad Stab. 1998; 60(2–3):247–51.
35. Nada A-AM, El-sakhawy M, Kamel S. Modified kraft pulping of bagasse: infrared spectroscopy of lignin. Int J Polym Mater. 2000;46(1–2):121–30.
36. Peredo K, Escobar D, Vega-Lara J, Berg A, Pereira M. Thermochemical properties of cellulose acetate blends with acetosolv and sawdust lignin: a comparative study. Int J Biol Macromol. 2016;83:403–9. doi:10.1016/j.ijbiomac.2015.11.022.
37. Reza M, Kontturi E, Jääskeläinen A-S, Vuorinen T, Ruokolainen J. Transmission electron microscopy for wood and fiber analysis–a review. BioResources. 2015;10(3):6230–61. doi:10.15376/biores.
38. Pan X, Kadla JF, Ehara K, Gilkes N, Saddler JN. Organosolv ethanol lignin from hybrid poplar as a radical scavenger: relationship between lignin structure, extraction conditions, and antioxidant activity. J Agric Food Chem. 2006;54(16):5806–13. doi:10.1021/jf0605392.
39. Hasan M, Lai TK, Chong EWN, Gopakumar DA, Rizal S, Hossain MS, et al. Organic and inorganic fillers' role on the amelioration of *Kappaphycus* spp.-based biopolymer films' performance. BioResources. 2019;14(4):9198–213. doi:10.15376/biores.
40. Iqhrammullah M, Marlina M, Khalil HA, Kurniawan K, Suyanto H, Hedwig R, et al. Characterization and performance evaluation of cellulose acetate-polyurethane film for lead II ion removal. Polymers. 2020;12(6):1317. doi:10.3390/polym12061317.
41. Zhou Y, Han Y, Xu J, Han W, Gu F, Sun K, et al. Strong, flexible and UV-shielding composite polyvinyl alcohol films with wood cellulose skeleton and lignin nanoparticles. Int J Biol Macromol. 2023;232:123105. doi:10.1016/j.ijbiomac.2022.12.324.
42. Abdullah R, Astira D, Zulfiani U, Widyanto AR, Hidayat ARP, Sulistiono DO, et al. Fabrication of composite membrane with microcrystalline cellulose from lignocellulosic biomass as filler on cellulose acetate based membrane for water containing methylene blue treatment. Biores Tech Rep. 2024;25:101728.